

JOINT-VAE: LEARNING DISENTANGLED JOINT CONTINUOUS AND DISCRETE REPRESENTATIONS

Emilien Dupont

Schlumberger Software Technology Innovation Center
Menlo Park, CA, USA
dupont@slb.com

ABSTRACT

We present a framework for learning disentangled and interpretable jointly continuous and discrete representations in an unsupervised manner. By augmenting the continuous latent distribution of variational autoencoders with a relaxed discrete distribution and controlling the amount of information encoded in each latent unit, we show how continuous and categorical factors of variation can be discovered automatically from data. The learned model also contains an inference network which can infer quantities such as angle and width of objects from image data in a completely unsupervised manner. Our experiments show that the framework disentangles continuous and discrete generative factors on various datasets, including disentangling digit type from stroke thickness, angle and width on MNIST, chair type from azimuth and width on the Chairs dataset and age from azimuth on CelebA.

1 INTRODUCTION

Disentangled representations are defined as ones where a change in a single unit of the representation corresponds to a change in single factor of variation of the data while being invariant to others (Bengio et al. (2013)). For example, a disentangled representation of 3D objects should contain a set of units each corresponding to a generative factor such as position, lighting, color or scale (see Fig. 1).

A large number of machine learning tasks, with transfer learning being the most prominent, can benefit from disentangled representations (Lake et al. (2017)). In addition, disentangled representations have recently been used in reinforcement learning (Higgins et al. (2017a)) and for learning visual concepts (Higgins et al. (2017b)). In contrast to most representation learning algorithms which encode data in complicated non interpretable ways, disentangled representations are often interpretable since they align with factors of variation of the data.

Several approaches have been explored for semi-supervised or supervised learning of factored representations (Kulkarni et al. (2015); Whitney et al. (2016); Yang et al. (2015); Reed et al. (2014)).



Figure 1: Disentanglement and entanglement on images of chairs. The first row shows a disentangled representation, varying a unit of the representation only alters one generative factor (azimuth) while others remain fixed. The second row shows an entangled representation where varying a unit of the representation does not correspond to a single generative factor but a mix of azimuth, chair type and size.

These approaches achieve impressive results but either require knowledge of the underlying generative factors or other forms of weak supervision. Several methods also exist for unsupervised disentanglement with the two most prominent being InfoGAN and β -VAE (Desjardins et al. (2012); Chen et al. (2016); Higgins et al. (2016)). These frameworks have shown promise in disentangling factors of variation in an unsupervised manner on a number of datasets.

InfoGAN (Chen et al. (2016)) is a framework based on Generative Adversarial Networks (Goodfellow et al. (2014)) which disentangles generative factors by maximizing the mutual information between a subset of latent variables and the generated samples. While this approach is able to model both discrete and continuous factors, it suffers from some of the shortcomings of Generative Adversarial Networks (GAN), such as unstable training and reduced sample diversity. Recent improvements in the training of GANs (Arjovsky et al. (2017); Gulrajani et al. (2017)) have mitigated some of these issues, but stable GAN training still remains a challenge. β -VAE (Higgins et al. (2016)), in contrast, is based on Variational Autoencoders (Kingma & Welling (2013); Rezende et al. (2014)) and is stable to train. β -VAE, however, can only model continuous latent variables.

In this paper we propose a framework, based on Variational Autoencoders (VAE), that learns disentangled continuous and discrete representations in an unsupervised manner. It comes with the advantages of VAEs, such as stable training, large sample diversity and a principled inference network, while having the flexibility to model a combination of continuous and discrete generative factors. We show how our framework, which we term Joint-VAE, discovers independent factors of variation on MNIST, FashionMNIST (Xiao et al. (2017)), CelebA (Liu et al. (2015)) and Chairs (Aubry et al. (2014)). For example, on MNIST, Joint-VAE disentangles digit type (discrete) from slant, width and stroke thickness (continuous). On CelebA, it disentangles azimuth, hair color and age. In addition, the model’s learned inference network can infer various properties of data in an unsupervised manner. For example, it infers angle of rotation of a chair from raw pixel data in a completely unsupervised manner. Finally, the inference network can be used for simple image editing, such as rotating a face in an image.

2 ANALYSIS OF β -VAE

We derive our approach by modifying the β -VAE framework and augmenting it with a joint latent distribution. β -VAEs model a joint distribution of the data \mathbf{x} and a set of latent variables \mathbf{z} and learn continuous disentangled representations by maximizing the objective

$$\mathcal{L}(\theta, \phi) = \mathbb{E}_{q_\phi(\mathbf{z}|\mathbf{x})}[\log p_\theta(\mathbf{x}|\mathbf{z})] - \beta D_{KL}(q_\phi(\mathbf{z}|\mathbf{x}) \parallel p(\mathbf{z})) \quad (1)$$

where the posterior or encoder $q_\phi(\mathbf{z}|\mathbf{x})$ is a neural network with parameters ϕ mapping \mathbf{x} into \mathbf{z} , the likelihood or decoder $p_\theta(\mathbf{x}|\mathbf{z})$ is a neural network with parameters θ mapping \mathbf{z} into \mathbf{x} and β is a positive constant. The loss is a weighted sum of a likelihood term $\mathbb{E}_{q_\phi(\mathbf{z}|\mathbf{x})}[\log p_\theta(\mathbf{x}|\mathbf{z})]$ which encourages the model to encode the data \mathbf{x} into a set of latent variables \mathbf{z} which can efficiently reconstruct the data and a second term that encourages the distribution of the inferred latents \mathbf{z} to be close to some prior $p(\mathbf{z})$. When $\beta = 1$, this corresponds to the original VAE framework. However, when $\beta > 1$, it is theorized that the increased pressure of the posterior $q_\phi(\mathbf{z}|\mathbf{x})$ to match the prior $p(\mathbf{z})$, combined with maximizing the likelihood term, gives rises to efficient and disentangled representations of the data (Higgins et al. (2016); Burgess et al. (2017)).

We can derive further insights by analyzing the role of the KL divergence term in the objective (1). During training, the objective will be optimized in expectation over the data \mathbf{x} . The KL term then becomes (Makhzani & Frey (2017); Kim & Mnih (2018))

$$\begin{aligned} \mathbb{E}_{p(\mathbf{x})}[D_{KL}(q_\phi(\mathbf{z}|\mathbf{x}) \parallel p(\mathbf{z}))] &= I(\mathbf{x}; \mathbf{z}) + D_{KL}(q(\mathbf{z}) \parallel p(\mathbf{z})) \\ &\geq I(\mathbf{x}; \mathbf{z}) \end{aligned} \quad (2)$$

i.e., when taken in expectation over the data, the KL divergence term is an upper bound on the mutual information between the latents and the data (see appendix A.1 for proof and details). Thus, a mini batch estimate of the mean KL divergence is an estimate of the upper bound on the information \mathbf{z} can transmit about \mathbf{x} . As such, the β -VAE objective puts a stronger constraint on the amount

of information \mathbf{z} can transmit about \mathbf{x} than the traditional VAE framework, while maintaining the pressure of maximizing the log likelihood.

Penalizing the mutual information term improves disentanglement but comes at the cost of increased reconstruction error. Recently, several methods have been explored to improve the reconstruction quality without decreasing disentanglement (Burgess et al. (2017); Kim & Mnih (2018)). Burgess et al. (2017) in particular propose an objective where the upper bound on the mutual information is controlled and gradually increased during training. Denoting the controlled information capacity by C , the objective is defined as

$$\mathcal{L}(\theta, \phi) = \mathbb{E}_{q_\phi(\mathbf{z}|\mathbf{x})}[\log p_\theta(\mathbf{x}|\mathbf{z})] - \gamma |D_{KL}(q_\phi(\mathbf{z}|\mathbf{x}) \parallel p(\mathbf{z})) - C| \quad (3)$$

where γ is a constant which forces the KL divergence term to match the capacity C . Gradually increasing C during training allows for control of the amount of information the model can encode. This objective has been shown to improve reconstruction quality as compared to (1) without reducing disentanglement (Burgess et al. (2017)).

3 JOINT-VAE MODEL

We propose a modification to the β -VAE framework which allows us to model a joint distribution of continuous and discrete latent variables. Letting \mathbf{z} denote a set of continuous latent variables and \mathbf{c} denote a set of categorical or discrete latent variables, we define a joint posterior $q_\phi(\mathbf{z}, \mathbf{c}|\mathbf{x})$, prior $p(\mathbf{z}, \mathbf{c})$ and likelihood $p_\theta(\mathbf{x}|\mathbf{z}, \mathbf{c})$. The β -VAE objective then becomes

$$\mathcal{L}(\theta, \phi) = \mathbb{E}_{q_\phi(\mathbf{z}, \mathbf{c}|\mathbf{x})}[\log p_\theta(\mathbf{x}|\mathbf{z}, \mathbf{c})] - \beta D_{KL}(q_\phi(\mathbf{z}, \mathbf{c}|\mathbf{x}) \parallel p(\mathbf{z}, \mathbf{c})) \quad (4)$$

where the latent distribution is now jointly continuous and discrete. Assuming the continuous and discrete latent variables are conditionally independent¹, i.e. $q_\phi(\mathbf{z}, \mathbf{c}|\mathbf{x}) = q_\phi(\mathbf{z}|\mathbf{x})q_\phi(\mathbf{c}|\mathbf{x})$ and similarly for the prior $p(\mathbf{z}, \mathbf{c}) = p(\mathbf{z})p(\mathbf{c})$ we can rewrite the KL divergence as

$$D_{KL}(q_\phi(\mathbf{z}, \mathbf{c}|\mathbf{x}) \parallel p(\mathbf{z}, \mathbf{c})) = D_{KL}(q_\phi(\mathbf{z}|\mathbf{x}) \parallel p(\mathbf{z})) + D_{KL}(q_\phi(\mathbf{c}|\mathbf{x}) \parallel p(\mathbf{c})) \quad (5)$$

i.e. we can separate the discrete and continuous KL divergence terms (see appendix A.2 for proof). Under this assumption, the loss becomes

$$\mathcal{L}(\theta, \phi) = \mathbb{E}_{q_\phi(\mathbf{z}, \mathbf{c}|\mathbf{x})}[\log p_\theta(\mathbf{x}|\mathbf{z}, \mathbf{c})] - \beta D_{KL}(q_\phi(\mathbf{z}|\mathbf{x}) \parallel p(\mathbf{z})) - \beta D_{KL}(q_\phi(\mathbf{c}|\mathbf{x}) \parallel p(\mathbf{c})) \quad (6)$$

Instead of directly optimizing this loss, we gradually increase the channel capacity as in equation (3). The capacities of the discrete and continuous latent channels are controlled separately forcing the model to encode information both in the discrete and continuous channels. The final loss is then given by

$$\mathcal{L}(\theta, \phi) = \mathbb{E}_{q_\phi(\mathbf{z}, \mathbf{c}|\mathbf{x})}[\log p_\theta(\mathbf{x}|\mathbf{z}, \mathbf{c})] - \gamma_z |D_{KL}(q_\phi(\mathbf{z}|\mathbf{x}) \parallel p(\mathbf{z})) - C_z| - \gamma_c |D_{KL}(q_\phi(\mathbf{c}|\mathbf{x}) \parallel p(\mathbf{c})) - C_c| \quad (7)$$

where C_z and C_c are gradually increased during training.

3.1 PARAMETRIZATION OF CONTINUOUS LATENT VARIABLES

As in the original VAE framework, we parametrize $q_\phi(\mathbf{z}|\mathbf{x})$ by a factorised Gaussian, i.e. $q_\phi(\mathbf{z}|\mathbf{x}) = \prod_i q_\phi(z_i|\mathbf{x})$ where $q_\phi(z_i|\mathbf{x}) = \mathcal{N}(\mu_i, \sigma_i^2)$ and let the prior be a unit Gaussian $p(\mathbf{z}) = \mathcal{N}(0, I)$. $\boldsymbol{\mu}$ and $\boldsymbol{\sigma}^2$ are both parametrized by neural networks.

¹Note that in this framework, as in the original VAE framework, *all* latent variables are conditionally independent. However, for the sake of deriving the Joint-VAE objective we only require conditional independence between the continuous and discrete latents.

3.2 PARAMETRIZATION OF DISCRETE LATENT VARIABLES

Parametrizing $q_\phi(\mathbf{c}|\mathbf{x})$ is more difficult. Since $q_\phi(\mathbf{c}|\mathbf{x})$ needs to be differentiable with respect to its parameters, we cannot parametrize $q_\phi(\mathbf{c}|\mathbf{x})$ by a set of categorical distributions. Recently, Maddison et al. (2016) and Jang et al. (2016) proposed a differentiable relaxation of discrete random variables based on the Gumbel Max trick (Gumbel (1954)). If c is a categorical variable with class probabilities $\alpha_1, \alpha_2, \dots, \alpha_n$, then we can sample from a continuous approximation of the categorical distribution, by sampling a set of $g_k \sim \text{Gumbel}^2$ i.i.d. and applying the following transformation

$$y_k = \frac{\exp((\log \alpha_k + g_k)/\tau)}{\sum_i \exp((\log \alpha_i + g_i)/\tau)} \quad (8)$$

where τ is a temperature parameter which controls the relaxation. The sample \mathbf{y} is a continuous approximation of the one hot representation of \mathbf{c} . The relaxed discrete distribution is called a Concrete or Gumbel Softmax distribution and is denoted by $g(\boldsymbol{\alpha})$ where $\boldsymbol{\alpha}$ is a vector of class probabilities.

We can parametrize $q_\phi(\mathbf{c}|\mathbf{x})$ by a product of independent Gumbel Softmax distributions, $q_\phi(\mathbf{c}|\mathbf{x}) = \prod_i q_\phi(c_i|\mathbf{x})$ where $q_\phi(c_i|\mathbf{x}) = g(\boldsymbol{\alpha}^{(i)})$ is a Gumbel Softmax distribution with class probabilities $\boldsymbol{\alpha}^{(i)}$. We let the prior $p(\mathbf{c})$ be equal to a product of uniform Gumbel Softmax distributions. This approach allows us to use the reparametrization trick (Kingma & Welling (2013); Rezende et al. (2014)) and efficiently train the discrete model.

3.3 ARCHITECTURE

The final architecture of the Joint-VAE model is shown in Fig. 2. We build the encoder to output the parameters of the continuous distribution $\boldsymbol{\mu}$ and $\boldsymbol{\sigma}^2$ and of each of the discrete distributions $\boldsymbol{\alpha}^{(i)}$. We then sample $z_i \sim \mathcal{N}(\mu_i, \sigma_i^2)$ and $c_i \sim g(\boldsymbol{\alpha}^{(i)})$ using the reparametrization trick and concatenate \mathbf{z} and \mathbf{c} into one latent vector which is passed as input to the decoder.

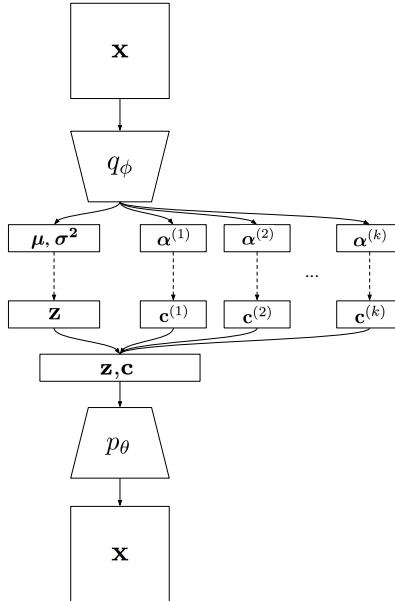


Figure 2: Joint-VAE architecture. The input \mathbf{x} is encoded by q_ϕ into the parameters of the latent distributions. Samples are drawn from each of the latent distributions using the reparametrization trick (indicated by dashed arrows on the diagram). The samples are then concatenated and decoded through p_θ .

²The Gumbel distribution can be sampled by drawing $u \sim \text{Uniform}(0,1)$ and computing $g = -\log(-\log(u))$

4 EXPERIMENTS

We perform experiments on several datasets including MNIST, FashionMNIST, CelebA and Chairs. We parametrize the encoder by a convolutional neural network and the decoder by the same network, transposed (for the full architecture and training details see appendix).

MNIST

Disentanglement results and latent traversals for MNIST are shown in Fig. 3. The model was trained with 10 continuous latent variables and one discrete 10-dimensional latent variable. The model discovers several factors of variation in the data, such as digit type (discrete), stroke thickness, angle and width (continuous) in an unsupervised manner. As can be seen from the latent traversals in Fig. 3, the trained model is able to generate realistic samples for a large variety of latent settings. Fig. 4 shows digits generated by fixing the discrete latent and sampling the continuous latents from the prior $p(\mathbf{z}) = \mathcal{N}(0, 1)$, which can be interpreted as sampling from a distribution conditioned on digit type. As can be seen, the samples are diverse and realistic and honor the conditioning.

For a large range of hyperparameters we were not able to achieve disentanglement using the purely continuous β -VAE framework. This is likely because MNIST has an inherently discrete generative factor (digit type), which β -VAE is unable to map onto a continuous latent variable. In contrast, the Joint-VAE approach allows us to disentangle the discrete factors while maintaining disentanglement of continuous factors.

FASHIONMNIST

Latent traversals for FashionMNIST are shown in Fig. 5. We also used 10 continuous and 1 discrete latent variable for this dataset. FashionMNIST is much harder to disentangle as the generative factors for creating clothes are less clear than the ones for drawing digits. However, Joint-VAE performs well and discovers interesting dimensions, such as sleeve length, heel size and shirt color. As some of the classes of FashionMNIST are very similar (e.g. shirt and t-shirt are two different classes), not all classes are discovered. However, a significant amount of them are disentangled including dress, t-shirt, trousers, sneakers, bag, ankle boot and so on (see Fig. 4).

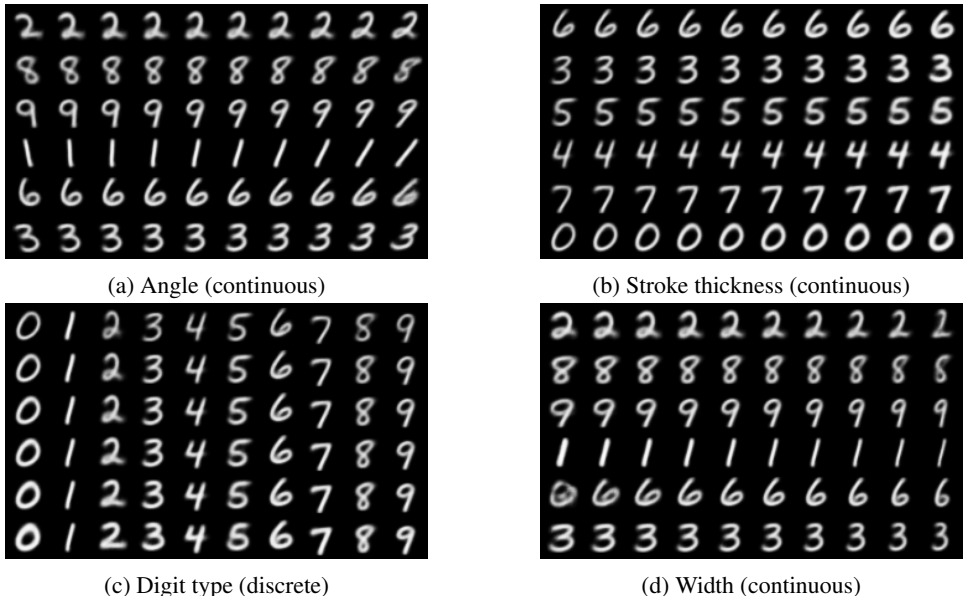


Figure 3: Latent traversals of the model trained on MNIST with 10 continuous latent variables and 1 discrete latent variable. Each row corresponds to a fixed random setting of the latent variables and the columns correspond to varying a single latent unit. Each subfigure varies a different latent unit. As can be seen each of the varied latent units corresponds to an interpretable generative factor, such as stroke thickness or digit type.

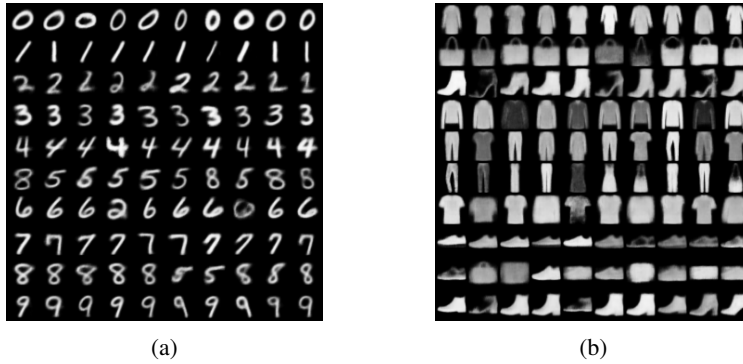


Figure 4: (a) Samples conditioned on digit type. Each row shows samples from p_θ where the discrete latent variable is fixed and all other latent values are sampled from the prior. As can be seen each row produces diverse samples of each digit. Note that digits which are similar, such as 5 and 8 are sometimes confused and not perfectly disentangled. (b) Samples conditioned on fashion item type. The samples are diverse and largely disentangled.

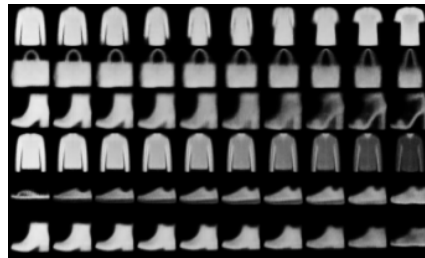


Figure 5: Latent traversals of FashionMNIST model. The rows correspond to different settings of the discrete latent variable, while the columns correspond to a traversal of the most informative continuous latent variable. Various factors are discovered, such as sleeve length, bag handle size, ankle height and shoe opening.

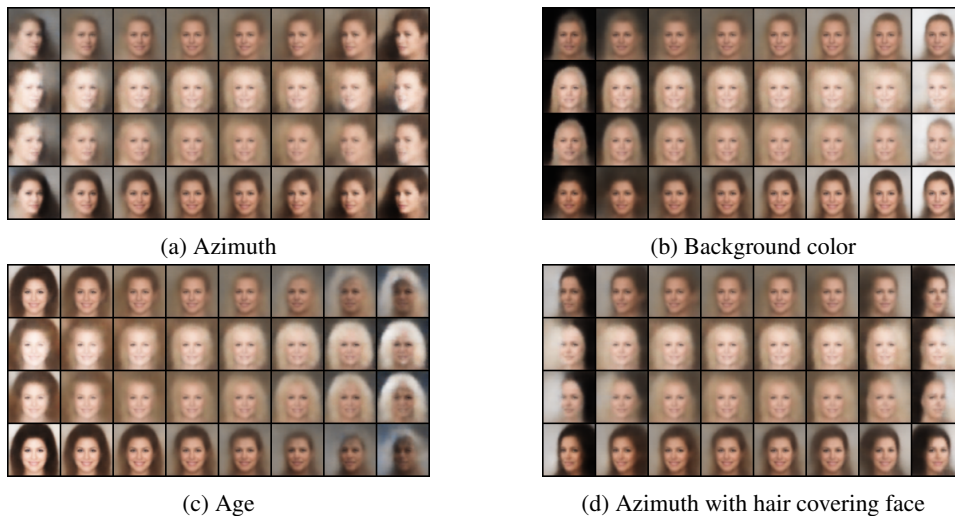


Figure 6: Latent traversals of the model trained on CelebA with 32 continuous latent variables and 1 discrete latent variable. Each row corresponds to a fixed setting of the discrete latent variables and the columns correspond to varying a single continuous latent unit.

CELEBA

For CelebA we used a model with 32 continuous latent variables and one 10 dimensional discrete latent variable. As shown in Fig. 6, the Joint-VAE model discovers various factors of variation including azimuth, age and hair color, while being able to generate realistic samples. While the samples are not as sharp as those produced by entangled models, we can still see details in the images such as distinct facial features and skin tones. Different settings of the discrete variable correspond to different facial identities.

CHAIRS

For the chairs dataset we used a model with 32 continuous latent variables and one 10 dimensional discrete latent variable. Joint-VAE discovers several factors of variation such as chair rotation and width. Furthermore, different settings of the discrete variable correspond to different chair types.

4.1 DETECTING DISENTANGLEMENT IN LATENT DISTRIBUTIONS

As noted in Section 2, taken in expectation over data, the KL divergence between the inferred latents $q_\phi(\mathbf{z}, \mathbf{c}|\mathbf{x})$ and the priors, upper bounds the mutual information between the latent units and the data. Motivated by this, we can plot the KL divergence values for each latent unit averaged over a mini batch of data during training. As various factors of variation are discovered in the data, we would expect the KL divergence of the corresponding latent units to increase. This is shown in Fig. 7. As the capacities C_z and C_c are increased the model is able to encode more and more factors of variation. For MNIST, the first factor to be discovered is digit type, followed by angle and width. This is likely because encoding digit type results in the largest reconstruction error reduction, followed by encoding angle and width and so on.

After training, we can also measure the KL divergence of each latent unit on test data and rank the latent units by their average KL values. This corresponds to ranking the latent units by their information content, or by how much information they are transmitting about \mathbf{x} . Fig. 8 shows the ranked latent units for MNIST and Chairs along with a latent traversal of each unit. As can be seen, the latent units with large information content encode various aspects of the data while latent units with approximately zero KL divergence do not affect the output.

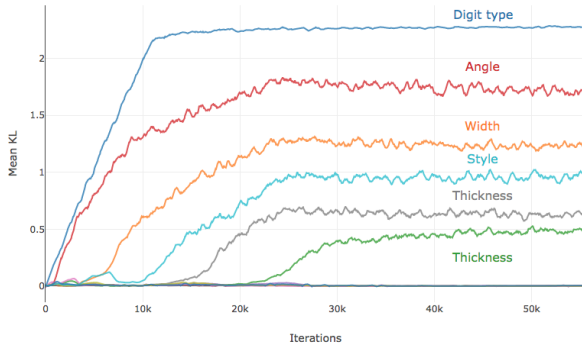


Figure 7: Increase of KL divergence during training. As the latent channel capacity is increased, different factors of variation are discovered. Most of the latent units have a KL divergence of approximately zero throughout training, meaning they do not encode any information about the data. As training progresses, however, some latent units start encoding more information about the data. Each latent unit can then be matched to a factor of variation of the data by visual inspection.

4.2 THE INFERENCE NETWORK

One of the advantages of Joint-VAE is that it comes with an inference network $q_\phi(\mathbf{z}, \mathbf{c}|\mathbf{x})$. For example, on MNIST we can infer the digit type on test data with 88.7% accuracy by simply looking at the value of the discrete latent variable $q_\phi(\mathbf{c}|\mathbf{x})$. Of course, this is completely unsupervised and the accuracy could likely be increased dramatically by using some label information.

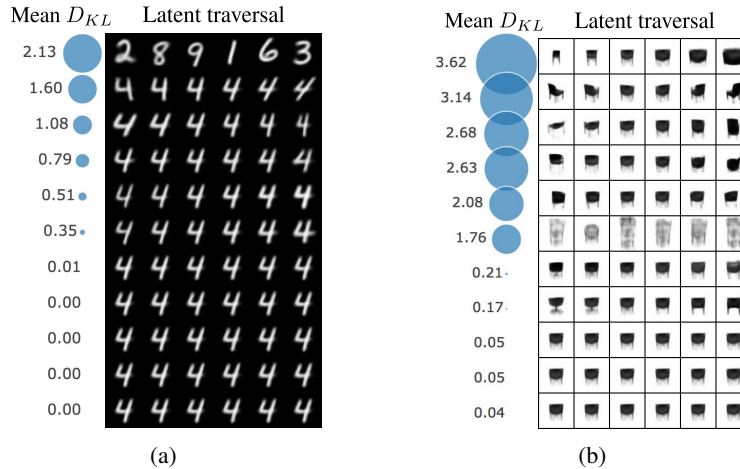


Figure 8: Each row corresponds to a latent traversal of a single latent unit. The column on the left shows the mean KL divergence value over a large number of examples (which corresponds to the amount of information encoded in that latent unit in nats). The rows are ordered from the latent unit with largest KL divergence to the lowest. As can be seen large KL divergence values correspond to active latents which encode information about the data, whereas low KL divergence value channels do not affect the data.

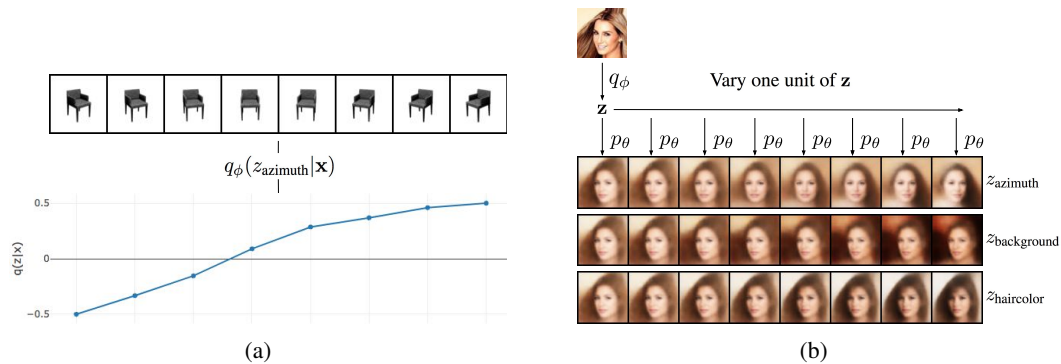


Figure 9: (a) Inference of azimuth on test data of chairs. The first row shows images of chairs from a test set. The second row shows the inferred z for each of the images. As can be seen, the latent unit successfully identifies rotation. (b) Image editing with Joint-VAE. An image of a celebrity is encoded with q_ϕ . In the encoded space, we can then rotate the face, change the background color or change the hair style by manipulating the latent unit corresponding to each factor. The bottom rows show the decoded images when each latent factor is changed. The samples are not as sharp as the original image, but these initial results show promise for using disentangled representations to edit images.

Since we are learning several generative factors, the inference network can also be used to infer properties which we do not have labels for. For example, the latent unit corresponding to azimuth on the chairs dataset correlates well with the actual azimuth of unseen chairs. After training a model on the chairs dataset and identifying the latent unit corresponding to azimuth, we can test the inference network on images that were not used during training. This is shown in Fig. 9a. As can be seen the latent unit corresponding to rotation infers the angle of the chair even though no labeled data was given (or available) for this task.

The framework can also be used to perform image editing or manipulation. If we wish to rotate the image of a face, we can encode the face with q_ϕ , modify the latent corresponding to azimuth and decode the resulting vector with p_θ . Examples of this are shown in Fig. 9b.

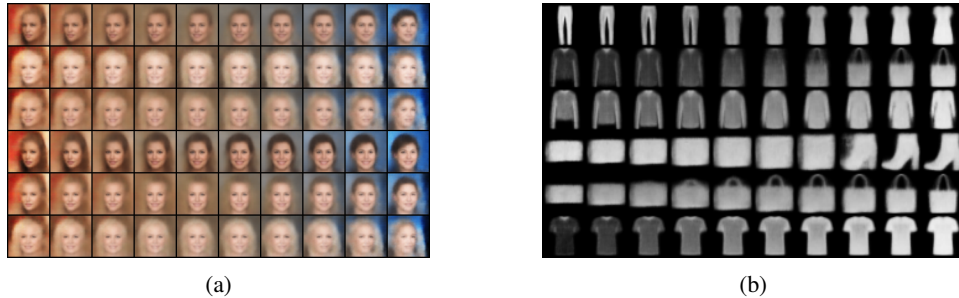


Figure 10: Failure examples. (a) Background color is entangled with azimuth and hair length. (b) Various clothing items are entangled with each other.

4.3 ROBUSTNESS AND SENSITIVITY TO HYPERPARAMETERS

As with most unsupervised disentanglement frameworks such as InfoGAN and β -VAE, Joint-VAE is sensitive to the choice of hyperparameters. Even with a good choice of hyperparameters, the quality of disentanglement may vary based on the random seed. In general, it is easy to achieve some degree of disentanglement for a large set of hyperparameters, but achieving complete clean disentanglement (e.g. perfectly separate digit type and other generative factors) can be difficult. It would be interesting to explore more principled approaches for choosing the latent capacities and how to increase them but we leave this for future work.

We have included failure examples in Fig. 10. One of the main failure modes we experienced was using a γ that is too low. This allowed the model to initially break the capacity constraint and encode several factors in an entangled manner to make reconstruction error gains.

5 CONCLUSION

We have proposed Joint-VAE, a framework for learning disentangled continuous and discrete representations in an unsupervised manner. The framework comes with the advantages of VAEs such as stable training and large sample diversity while being able to model complex jointly continuous and discrete generative factors. We have shown that Joint-VAE disentangles factors of variation on several datasets while producing realistic samples. In addition, the inference network can be used to infer unlabeled quantities on test data and to edit and manipulate images.

In future work, it would be interesting to combine to this approach with other recent developments in unsupervised disentanglement, such as FactorVAE (Kim & Mnih (2018)) or β -TCVAE (Chen et al. (2018)). Gaining a deeper understanding of how disentanglement depends on the latent channel capacities and how they are increased will likely provide insights to build more stable models. Finally, it would also be interesting to explore the use of other latent distributions since the framework allows the use of any joint distribution of reparametrizable random variables.

REFERENCES

- Martin Arjovsky, Soumith Chintala, and Léon Bottou. Wasserstein gan. *arXiv preprint arXiv:1701.07875*, 2017.
- Mathieu Aubry, Daniel Maturana, Alexei A Efros, Bryan C Russell, and Josef Sivic. Seeing 3d chairs: exemplar part-based 2d-3d alignment using a large dataset of cad models. In *Proceedings of the IEEE conference on computer vision and pattern recognition*, pp. 3762–3769, 2014.
- Yoshua Bengio, Aaron Courville, and Pascal Vincent. Representation learning: A review and new perspectives. *IEEE transactions on pattern analysis and machine intelligence*, 35(8):1798–1828, 2013.
- Christopher Burgess, Irina Higgins, Arka Pal, Loic Matthey, Nick Watters, Guillaume Desjardins, and Alexander Lerchner. Understanding disentangling in beta-vae. *NIPS 2017 Disentanglement Workshop*, 2017.

-
- Tian Qi Chen, Xuechen Li, Roger Grosse, and David Duvenaud. Isolating sources of disentanglement in variational autoencoders. *arXiv preprint arXiv:1802.04942*, 2018.
- Xi Chen, Yan Duan, Rein Houthoofd, John Schulman, Ilya Sutskever, and Pieter Abbeel. Infogan: Interpretable representation learning by information maximizing generative adversarial nets. In *Advances in Neural Information Processing Systems*, pp. 2172–2180, 2016.
- Guillaume Desjardins, Aaron Courville, and Yoshua Bengio. Disentangling factors of variation via generative entangling. *arXiv preprint arXiv:1210.5474*, 2012.
- Ian Goodfellow, Jean Pouget-Abadie, Mehdi Mirza, Bing Xu, David Warde-Farley, Sherjil Ozair, Aaron Courville, and Yoshua Bengio. Generative adversarial nets. In *Advances in neural information processing systems*, pp. 2672–2680, 2014.
- Ishaan Gulrajani, Faruk Ahmed, Martin Arjovsky, Vincent Dumoulin, and Aaron C Courville. Improved training of wasserstein gans. In *Advances in Neural Information Processing Systems*, pp. 5769–5779, 2017.
- Emil Julius Gumbel. Statistical theory of extreme value and some practical applications. *Nat. Bur. Standards Appl. Math. Ser. 33*, 1954.
- Irina Higgins, Loic Matthey, Arka Pal, Christopher Burgess, Xavier Glorot, Matthew Botvinick, Shakir Mohamed, and Alexander Lerchner. beta-vae: Learning basic visual concepts with a constrained variational framework. *ICLR 2017*, 2016.
- Irina Higgins, Arka Pal, Andrei A Rusu, Loic Matthey, Christopher P Burgess, Alexander Pritzel, Matthew Botvinick, Charles Blundell, and Alexander Lerchner. Darla: Improving zero-shot transfer in reinforcement learning. *arXiv preprint arXiv:1707.08475*, 2017a.
- Irina Higgins, Nicolas Sonnerat, Loic Matthey, Arka Pal, Christopher P Burgess, Matthew Botvinick, Demis Hassabis, and Alexander Lerchner. Scan: learning abstract hierarchical compositional visual concepts. *arXiv preprint arXiv:1707.03389*, 2017b.
- Eric Jang, Shixiang Gu, and Ben Poole. Categorical reparameterization with gumbel-softmax. *arXiv preprint arXiv:1611.01144*, 2016.
- Hyunjik Kim and Andriy Mnih. Disentangling by factorising. *arXiv preprint arXiv:1802.05983*, 2018.
- Diederik P Kingma and Max Welling. Auto-encoding variational bayes. *arXiv preprint arXiv:1312.6114*, 2013.
- Tejas D Kulkarni, William F Whitney, Pushmeet Kohli, and Josh Tenenbaum. Deep convolutional inverse graphics network. In *Advances in Neural Information Processing Systems*, pp. 2539–2547, 2015.
- Brenden M Lake, Tomer D Ullman, Joshua B Tenenbaum, and Samuel J Gershman. Building machines that learn and think like people. *Behavioral and Brain Sciences*, 40, 2017.
- Ziwei Liu, Ping Luo, Xiaogang Wang, and Xiaoou Tang. Deep learning face attributes in the wild. In *Proceedings of International Conference on Computer Vision (ICCV)*, 2015.
- Chris J Maddison, Andriy Mnih, and Yee Whye Teh. The concrete distribution: A continuous relaxation of discrete random variables. *arXiv preprint arXiv:1611.00712*, 2016.
- Alireza Makhzani and Brendan J Frey. Pixelgan autoencoders. In *Advances in Neural Information Processing Systems*, pp. 1972–1982, 2017.
- Scott Reed, Kihyuk Sohn, Yuting Zhang, and Honglak Lee. Learning to disentangle factors of variation with manifold interaction. In *International Conference on Machine Learning*, pp. 1431–1439, 2014.
- Danilo Jimenez Rezende, Shakir Mohamed, and Daan Wierstra. Stochastic backpropagation and approximate inference in deep generative models. *arXiv preprint arXiv:1401.4082*, 2014.

William F Whitney, Michael Chang, Tejas Kulkarni, and Joshua B Tenenbaum. Understanding visual concepts with continuation learning. *arXiv preprint arXiv:1602.06822*, 2016.

Han Xiao, Kashif Rasul, and Roland Vollgraf. Fashion-mnist: a novel image dataset for benchmarking machine learning algorithms. *arXiv preprint arXiv:1708.07747*, 2017.

Jimei Yang, Scott E Reed, Ming-Hsuan Yang, and Honglak Lee. Weakly-supervised disentangling with recurrent transformations for 3d view synthesis. In *Advances in Neural Information Processing Systems*, pp. 1099–1107, 2015.

A PROOFS

A.1 EXPECTATION OF KL DIVERGENCE AND MUTUAL INFORMATION

We can define the joint distribution of the data and the encoding distribution as $q(\mathbf{z}, \mathbf{x}) = p(\mathbf{x})q_\phi(\mathbf{z}|\mathbf{x})$. The distribution of the latent variables is then given by $q(\mathbf{z}) = \mathbb{E}_{p(\mathbf{x})}[q_\phi(\mathbf{z}|\mathbf{x})]$. We can now rewrite the KL divergence between the posterior and the prior taken in expectation over the data as

$$\begin{aligned}
 \mathbb{E}_{p(\mathbf{x})}[D_{KL}(q_\phi(\mathbf{z}|\mathbf{x}) \parallel p(\mathbf{z}))] &= \mathbb{E}_{p(\mathbf{x})}\mathbb{E}_{q_\phi(\mathbf{z}|\mathbf{x})}\left[\log \frac{q_\phi(\mathbf{z}|\mathbf{x})}{p(\mathbf{z})}\right] \\
 &= \mathbb{E}_{q(\mathbf{z}, \mathbf{x})}\left[\log \frac{q_\phi(\mathbf{z}|\mathbf{x})}{p(\mathbf{z})} \frac{q(\mathbf{z})}{q(\mathbf{z})}\right] \\
 &= \mathbb{E}_{q(\mathbf{z}, \mathbf{x})}\left[\log \frac{q_\phi(\mathbf{z}|\mathbf{x})}{q(\mathbf{z})}\right] + \mathbb{E}_{q(\mathbf{z}, \mathbf{x})}\left[\log \frac{q(\mathbf{z})}{p(\mathbf{z})}\right] \\
 &= \mathbb{E}_{q(\mathbf{z}, \mathbf{x})}\left[\log \frac{q(\mathbf{z}, \mathbf{x})}{q(\mathbf{z})p(\mathbf{x})}\right] + \mathbb{E}_{q(\mathbf{z})}\left[\log \frac{q(\mathbf{z})}{p(\mathbf{z})}\right] \\
 &= I(\mathbf{x}; \mathbf{z}) + D_{KL}(q(\mathbf{z}) \parallel p(\mathbf{z})) \\
 &\geq I(\mathbf{x}; \mathbf{z})
 \end{aligned}$$

where the mutual information is defined under the joint distribution of the data and the encoding distribution. Note that the last inequality follows because KL divergence is positive.

A.2 SPLITTING THE DISCRETE AND CONTINUOUS KL DIVERGENCE TERMS

Assuming the continuous and discrete latent variables are conditionally independent, i.e. $q_\phi(\mathbf{z}, \mathbf{c}|\mathbf{x}) = q_\phi(\mathbf{z}|\mathbf{x})q_\phi(\mathbf{c}|\mathbf{x})$ and similarly for the prior $p(\mathbf{z}, \mathbf{c}) = p(\mathbf{z})p(\mathbf{c})$ we can rewrite the joint KL divergence as

$$\begin{aligned}
 D_{KL}(q_\phi(\mathbf{z}, \mathbf{c}|\mathbf{x}) \parallel p(\mathbf{z}, \mathbf{c})) &= \mathbb{E}_{q_\phi(\mathbf{z}, \mathbf{c}|\mathbf{x})}\left[\log \frac{q_\phi(\mathbf{z}, \mathbf{c}|\mathbf{x})}{p(\mathbf{z}, \mathbf{c})}\right] \\
 &= \mathbb{E}_{q_\phi(\mathbf{z}|\mathbf{x})}\mathbb{E}_{q_\phi(\mathbf{c}|\mathbf{x})}\left[\log \frac{q_\phi(\mathbf{z}|\mathbf{x})q_\phi(\mathbf{c}|\mathbf{x})}{p(\mathbf{z})p(\mathbf{c})}\right] \\
 &= \mathbb{E}_{q_\phi(\mathbf{z}|\mathbf{x})}\mathbb{E}_{q_\phi(\mathbf{c}|\mathbf{x})}\left[\log \frac{q_\phi(\mathbf{z}|\mathbf{x})}{p(\mathbf{z})}\right] + \mathbb{E}_{q_\phi(\mathbf{z}|\mathbf{x})}\mathbb{E}_{q_\phi(\mathbf{c}|\mathbf{x})}\left[\log \frac{q_\phi(\mathbf{c}|\mathbf{x})}{p(\mathbf{c})}\right] \\
 &= \mathbb{E}_{q_\phi(\mathbf{z}|\mathbf{x})}\left[\log \frac{q_\phi(\mathbf{z}|\mathbf{x})}{p(\mathbf{z})}\right] + \mathbb{E}_{q_\phi(\mathbf{c}|\mathbf{x})}\left[\log \frac{q_\phi(\mathbf{c}|\mathbf{x})}{p(\mathbf{c})}\right] \\
 &= D_{KL}(q_\phi(\mathbf{z}|\mathbf{x}) \parallel p(\mathbf{z})) + D_{KL}(q_\phi(\mathbf{c}|\mathbf{x}) \parallel p(\mathbf{c}))
 \end{aligned}$$

B MODEL ARCHITECTURE

The architecture of the model is shown in the table below. The non linearities in both the encoder and decoder are ReLU except for the output layer of the decoder which is a sigmoid.

Encoder q_ϕ	Decoder p_θ
32 Conv 4×4 , stride 2	Linear latent dimension $\times 256$
32 Conv 4×4 , stride 2	Linear $256 \times 64 * 4 * 4$
64 Conv 4×4 , stride 2	64 Conv Transpose 4×4 , stride 2
64 Conv 4×4 , stride 2	32 Conv Transpose 4×4 , stride 2
Linear $64 * 4 * 4 \times 256$	32 Conv Transpose 4×4 , stride 2
Linear layers for parameters of each distribution	3 Conv Transpose 4×4 , stride 2

For 64 by 64 images (Chairs and CelebA) the above architecture was used. For 32 by 32 images (MNIST and FashionMNIST which were resized from 28 by 28) we used the same architecture with the last conv layer in the encoder and first in the decoder removed.

C TRAINING DETAILS

Parameters and training details for each model.

C.1 MNIST

- Latent distribution: 10 continuous, 1 10-dimensional discrete
- Optimizer: Adam with learning rate $5e-4$
- Batch size: 64
- Epochs: 100
- C_z : Increased linearly from 0 to 5 in 25000 iterations
- γ_z : 30
- C_c : Increased linearly from 0 to 5 in 25000 iterations
- γ_c : 30

C.2 FASHIONMNIST

- Latent distribution: 10 continuous, 1 10-dimensional discrete
- Optimizer: Adam with learning rate $5e-4$
- Batch size: 64
- Epochs: 100
- C_z : Increased linearly from 0 to 5 in 50000 iterations
- γ_z : 100
- C_c : Increased linearly from 0 to 10 in 50000 iterations
- γ_c : 100

C.3 CHAIRS

- Latent distribution: 32 continuous, 1 10-dimensional discrete
- Optimizer: Adam with learning rate $1e-4$
- Batch size: 64
- Epochs: 100
- C_z : Increased linearly from 0 to 30 in 100000 iterations
- γ_z : 300
- C_c : Increased linearly from 0 to 5 in 100000 iterations
- γ_c : 300

C.4 CELEBA

- Latent distribution: 32 continuous, 1 10-dimensional discrete
- Optimizer: Adam with learning rate $5e-4$
- Batch size: 64
- Epochs: 100
- C_z : Increased linearly from 0 to 50 in 100000 iterations
- γ_z : 100
- C_c : Increased linearly from 0 to 10 in 100000 iterations
- γ_c : 100